**Cell Reports, Volume *43***

## Supplemental information

# The nociceptive activity of peripheral sensory neurons is modulated by the neuronal membrane proteasome

**Eric Villalón Landeros, Samuel C. Kho, Taylor R. Church, Anna Brennan, Fulya Türker, Michael Delannoy, Michael J. Caterina, and Seth S. Margolis**

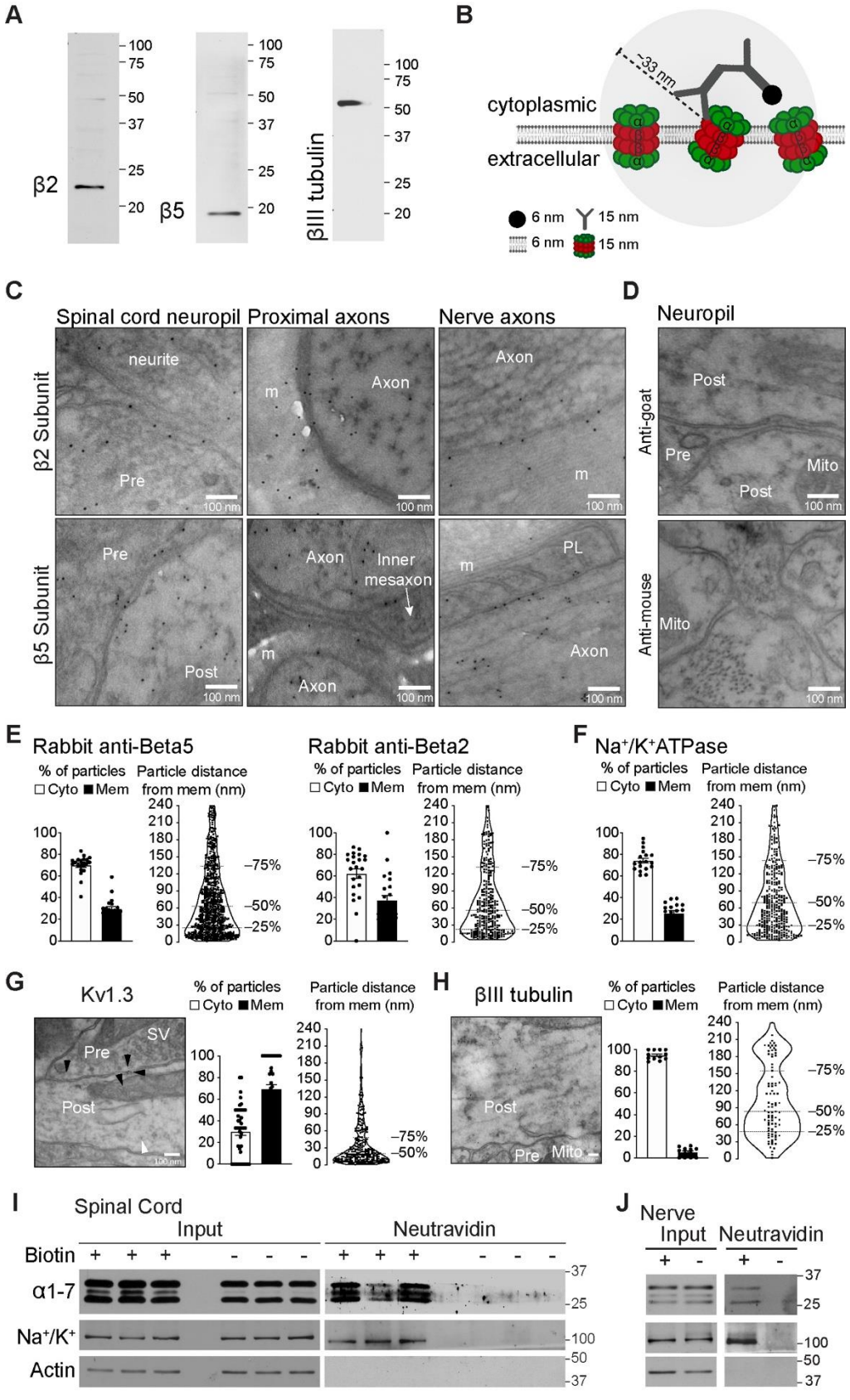
A
β2
β5
βIII tubulin
100
75
50
37
25
20
B
33 nm
cytoplasmic
extracellular
6 nm
15 nm
C
Spinal cord neuropil
Proximal axons
Nerve axons
β2 Subunit
β5 Subunit
neurite
Pre
Axon
m
Inner mesaxon
PL
Post
100 nm
D
Neuropil
Anti-goat
Anti-mouse
Post
Pre
Mito
E
Rabbit anti-Beta5
Rabbit anti-Beta2
% of particles
□Cyto ■Mem
Particle distance from mem (nm)
–75%
–50%
–25%
F
Na⁺/K⁺ATPase
G
Kv1.3
SV
H
βIII tubulin
I
Spinal Cord
Input
Neutravidin
Biotin
α1-7
Na⁺/K⁺
Actin
J
Nerve

**Figure S1. Related to Figure 1.**

**The NMP localizes to the membrane of PNS neurons**

(A) Proteasomes were detected using antibodies specific for the catalytic core subunits β2 and β5, and cytoplasmic control protein was detected using βIII-Tubulin antibodies.

(B) Schematic showing immuno-EM criteria used to detect proteasomes localizing on membranes.

(C) Representative images showing gold particle labeling of proteasomes on myelinated axons of the PNS. Each black dot on micrographs represents a gold particle that labels the localization of a proteasome. Myelin (m), pre-synaptic cell (pre), post-synaptic cell (post), synaptic vesicle (SV), mitochondria (Mito), paranodal loop (PL).

(D) Representative immuno-gold micrographs of no primary antibody control showing the lack of labeling on samples treated with only secondary conjugated anti-goat-6 nm and anti-mouse-6 nm.

(E) Quantification of gold particle localization using rabbit anti-β5 and rabbit anti-β2 antibodies (bar graphs) and gold particle distribution relative to the membrane (violin plots). Data presented as mean ± SEM (n = 20 - 30 micrographs analyzed from 2 independent animals).

(F) Quantification of gold particle localization using an antibody against $Na^+/K^+$-ATPase as membrane control (bar graph) and gold particle distribution relative to the membrane (violin plot). Data presented as mean ± SEM (n = 20 micrographs analyzed from 2 independent animals).

(G) Representative micrographs of immuno-gold labeling of membrane control protein, Kv1.3, and quantifications (bar graph and violin plot). Data presented as mean ± SEM (n = 35 micrographs analyzed from 2 independent animals).

(H) Representative micrographs and quantification (bar graph and violin plot) of immune-gold labeling of cytoplasmic control protein, βIII-tubulin. Data presented as mean ± SEM (n = 12 micrographs analyzed from 2 independent animals).

(I and J) Western blots of surface biotinylation and pulldown proteins from the spinal cord (I) and sciatic nerve (J) tissue from 1-month-old male mice. Input blots show detection of proteasome core proteins α1-7 subunits, membrane protein $Na^+/K^+$-ATPase, and cytosolic protein actin in both biotinylated and non-biotinylated samples. Western blots of neutravidin bead pulldown show the detection of core proteasome subunits α1-7 and membrane protein $Na^+/K^+$-ATPase in biotinylated samples but not in non-biotinylated tissues. Cytoplasmic control, actin, was not detected in pulldown protein pool. Western blots represent results obtained from multiple experiments with at least triplicate samples in each.

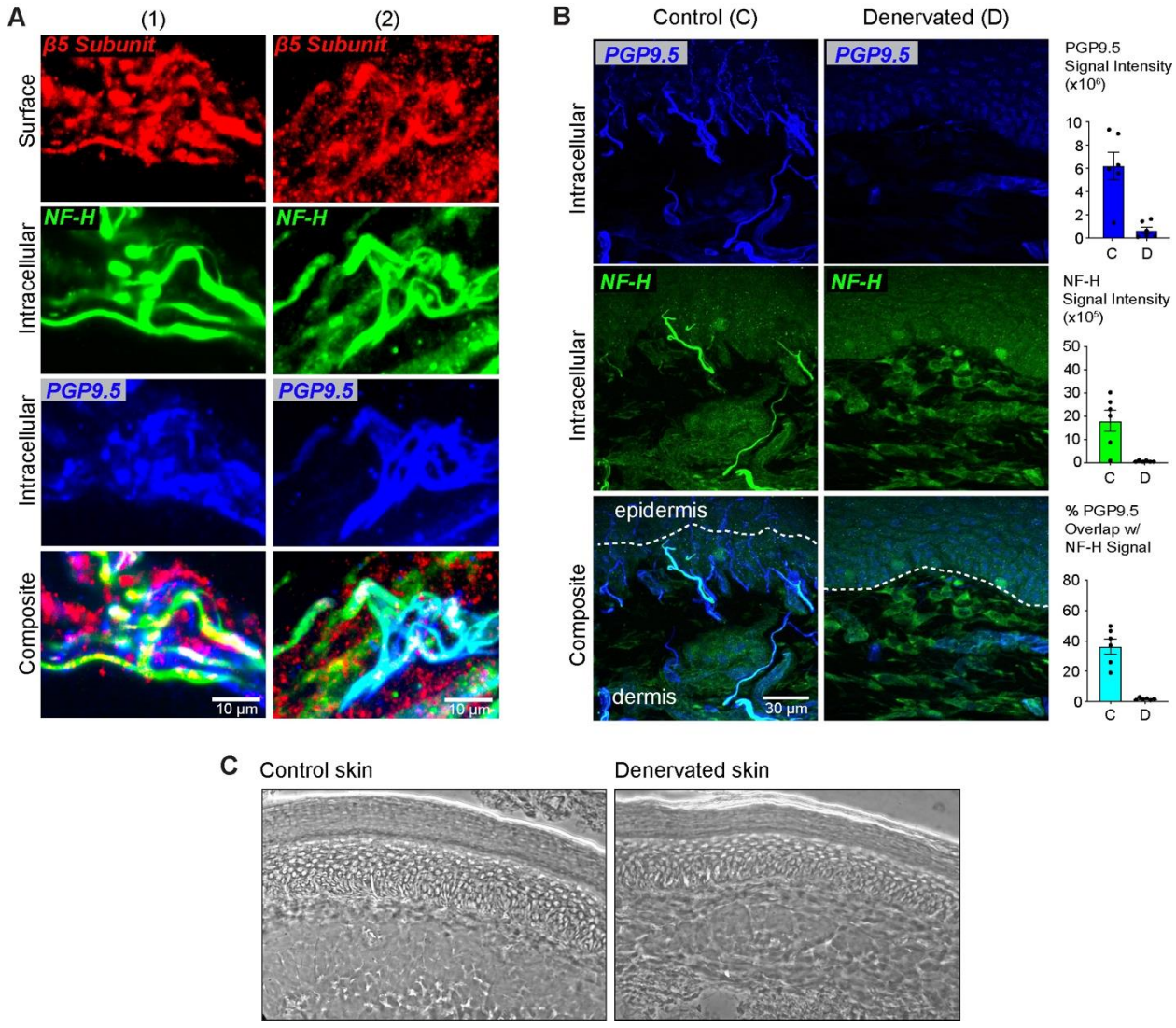
A
(1)
(2)
β5 Subunit
β5 Subunit
Surface
NF-H
NF-H
Intracellular
PGP9.5
PGP9.5
Intracellular
Composite
10 μm
10 μm
B
Control (C)
Denervated (D)
PGP9.5
PGP9.5
Intracellular
PGP9.5 Signal Intensity (x10⁶)
10
8
6
4
2
0
C
D
NF-H
NF-H
Intracellular
NF-H Signal Intensity (x10⁵)
50
40
30
20
10
0
C
D
epidermis
dermis
30 μm
Composite
% PGP9.5 Overlap w/ NF-H Signal
80
60
40
20
0
C
D
C
Control skin
Denervated skin

**Figure S2. Related to Figure 2.**

**Loss of paw skin innervation following nerve transection**

(A) Representative high resolution images of surface proteasome β5 subunit labeling (red) overlapping with nerve staining using NF-H (green) or PGP9.5 (blue) markers in the mouse hind paw skin.

(B) Representative images of mouse hind paw skin nerve staining in control and denervated paws. Denervation shows a lack of detectable nerve endings on the skin. Bar graphs (right) show quantifications of nerve staining intensity. Data are presented as mean ± SEM (n = 6 groups of images from 3 independent animals).

(C) Representative differential interference contrast (DIC) images of control and denervated paw skin sections used for NMP and nerve labeling. Note, denervation did not affect tissue integrity.

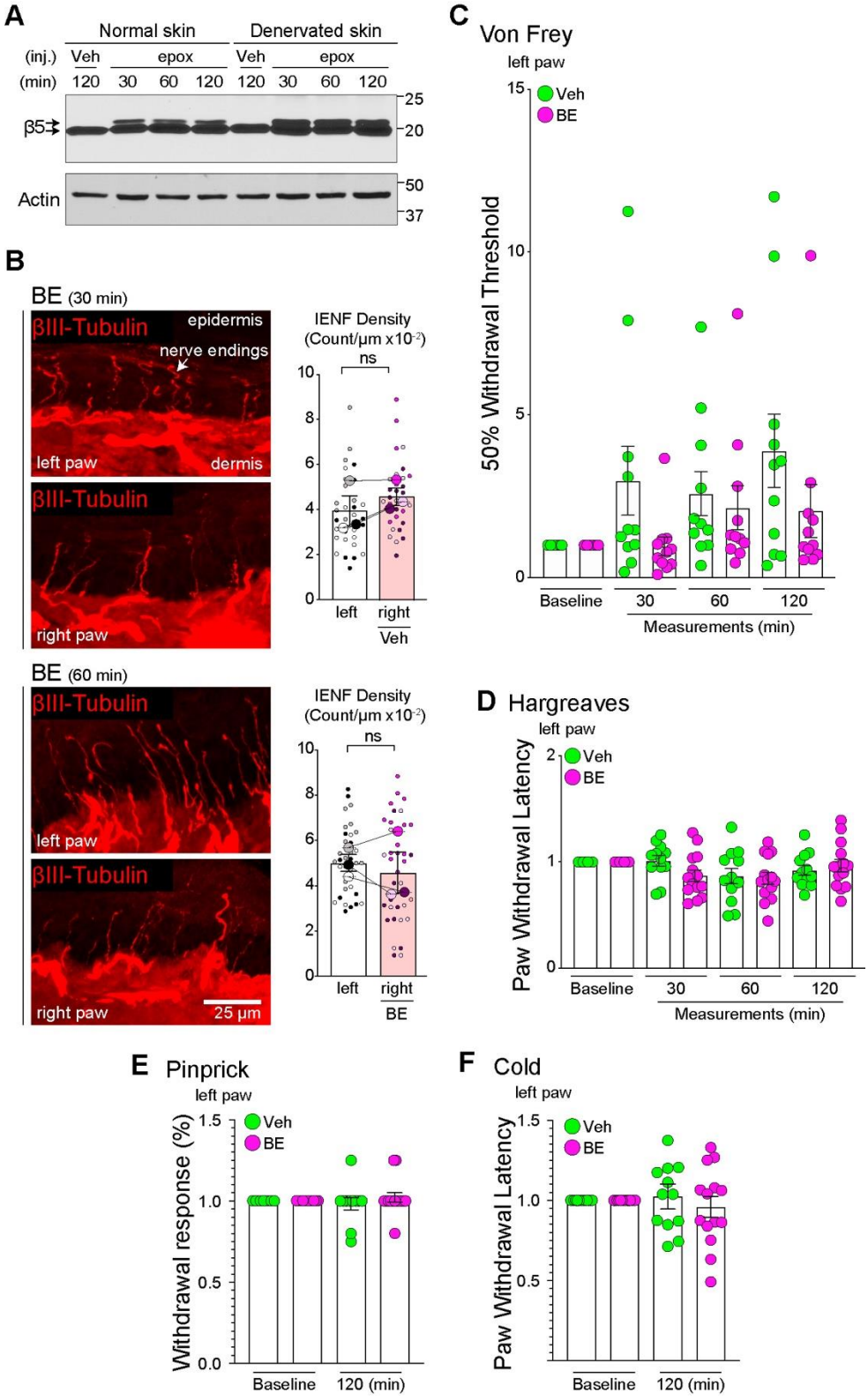
A
Normal skin
Denervated skin
(inj.) Veh epox Veh epox
(min) 120 30 60 120 120 30 60 120
β5
Actin
25
20
50
37
B
BE (30 min)
βIII-Tubulin
epidermis
nerve endings
left paw
dermis
right paw
IENF Density
(Count/μm x10-2)
ns
left
right
Veh
BE (60 min)
25 μm
BE
C
Von Frey
left paw
Veh
BE
50% Withdrawal Threshold
Baseline
30
60
120
Measurements (min)
D
Hargreaves
Paw Withdrawal Latency
E
Pinprick
Withdrawal response (%)
120 (min)
F
Cold

**Figure S3. Related to Figure 3.**

**Local and selective NMP inhibition does not affect nerve ending densities on paw skin**

(A) Western blotting of ipsilateral skin homogenates of paw skin treated with 10 μM epoxomicin, showing targeting of proteasome β5 subunits in both normal and denervated paw skin.

(B) Representative images of intraepidermal nerve fiber density in the skin after 30 and 60 min of BE injection into the right paw. Left paw was uninjected. Data are presented as mean ± SEM (n = 30 images analyzed). Statistically significant differences between samples was not observed (two-tailed t-test).

(C, D, E, F) Quantification of punctate mechanical (C), heat (D), painful mechanical (E), and noxious cold sensitivity (F) tests on the contralateral paw of mice injected with vehicle (Veh) or bio-epox (BE) at several time points post-injection. Data are presented as mean ± SEM (n = 14 (C), n = 10 - 12 (D), n = 14 (E), and n = 14 (F) mice per treatment). Statistically significant differences between samples was not observed (two-way ANOVA with a Tukey's post hoc test). All mouse behavior experiments data are normalized to baseline measurements per mouse.

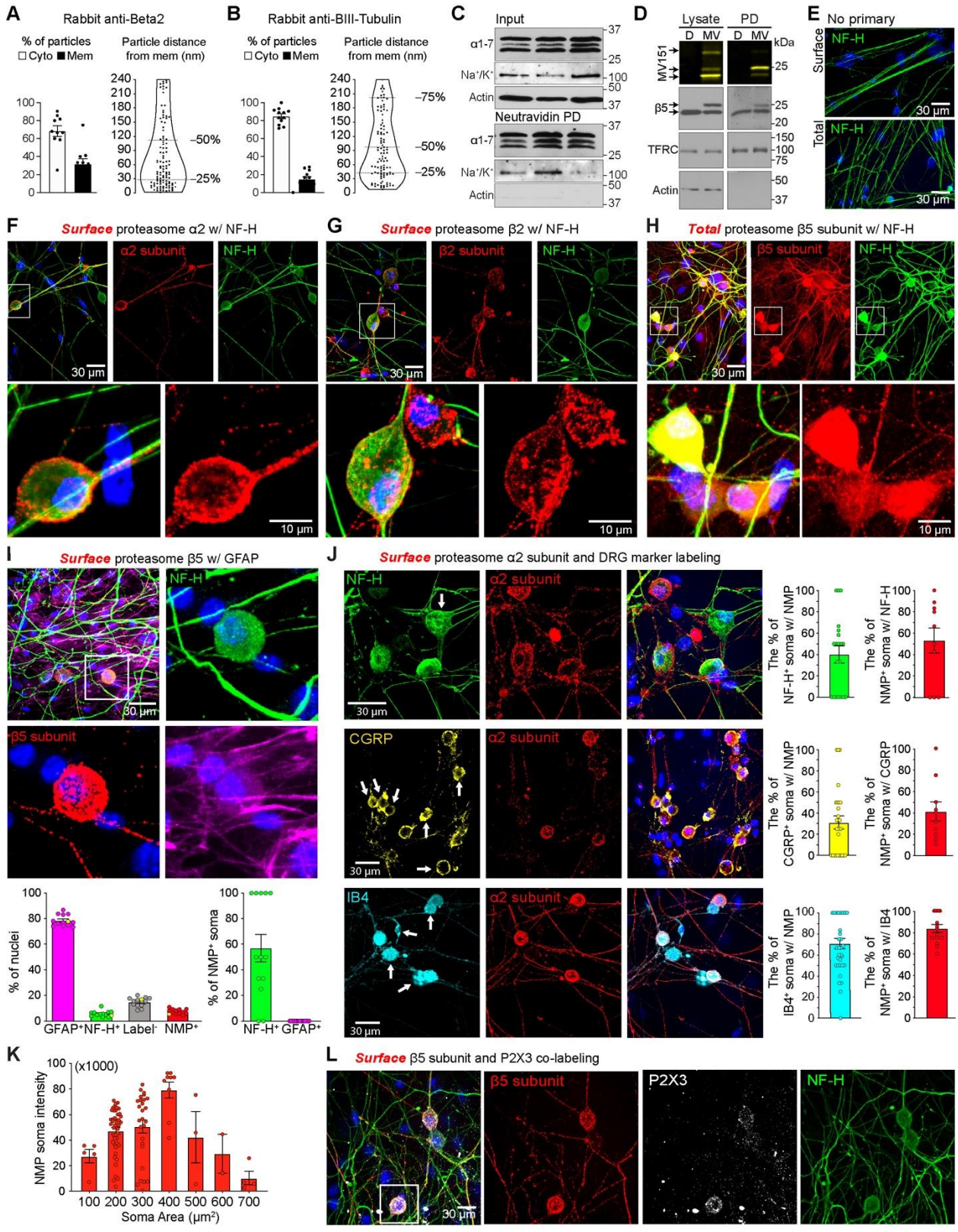
A
Rabbit anti-Beta2
% of particles
Cyto Mem
Particle distance from mem (nm)
–50%
–25%
B
Rabbit anti-BIII-Tubulin
% of particles
Cyto Mem
Particle distance from mem (nm)
–75%
–50%
–25%
C
Input
α1-7
Na+/K+
Actin
Neutravidin PD
α1-7
Na+/K+
Actin
D
Lysate
PD
D MV
D MV
kDa
MV151
β5
TFRC
Actin
E
No primary
Surface
Total
NF-H
30 μm
F
Surface proteasome α2 w/ NF-H
α2 subunit
NF-H
30 μm
10 μm
G
Surface proteasome β2 w/ NF-H
β2 subunit
NF-H
30 μm
10 μm
H
Total proteasome β5 subunit w/ NF-H
β5 subunit
NF-H
30 μm
10 μm
I
Surface proteasome β5 w/ GFAP
NF-H
β5 subunit
30 μm
% of nuclei
GFAP+ NF-H+ Label- NMP+
% of NMP+ soma
NF-H+ GFAP+
J
Surface proteasome α2 subunit and DRG marker labeling
NF-H
α2 subunit
CGRP
α2 subunit
IB4
α2 subunit
30 μm
The % of NF-H+ soma w/ NMP
The % of NMP+ soma w/ NF-H
The % of CGRP+ soma w/ NMP
The % of NMP+ soma w/ CGRP
The % of IB4+ soma w/ NMP
The % of NMP+ soma w/ IB4
K
NMP soma intensity
(x1000)
Soma Area (μm2)
L
Surface β5 subunit and P2X3 co-labeling
β5 subunit
P2X3
NF-H
30 μm

**Figure S4. Related to Figure 4.**

**Active NMPs localize on the somatic and axonal membranes of subgroups of DRG neurons**

(A) Quantification of immuno-EM proteasome localization in primary DRG cultures using an antibody against the β2 proteasome subunit (rabbit-anti-β2) showing gold particles localized to the cytoplasm (Cyto) and membrane (Mem) (bar graph). Violin plot demonstrates a high abundance of proteasomes on neuronal membranes and distribution of particles away from membranes. Data are presented as mean ± SEM (n = 10 micrographs analyzed).

(B) Immuno-EM particle localization analysis of βIII-tubulin as intracellular control protein showing 80-90% particles localize to the cytoplasm. Note: unlike proteasome subunits there are no particles for βIII-tubulin between 0 - 5 nm from the membrane. Data are presented as mean ± SEM (n = 12 micrographs analyzed).

(C) Western blot of surface biotinylation and pulldown proteins showing detection of α1-7 core subunits and membrane control $Na^+/K^+$-ATPase, but no cytoplasmic actin on neutravidin pulldown samples from cultured DRG neurons. Western blots represent experiments performed from several independent cultures in triplicates.

(D) Proteasome activity assay showing incorporation of activity-based probe, MV151, with catalytically active proteasome subunits in whole cell lysate and membrane pulldown fractions (top). Imaging was performed with a fluorescent gel imager. Immunoblotting for proteasome subunits shows shifting of the β5 proteasome subunit upon treatment with MV151 in whole cell lysate and membrane pulldown fractions (bottom). Membrane protein control TRFC was detected on both whole cell lysate and membrane fractions. Cytoplasmic protein, actin was only detected in whole cell lysate but not in membrane fraction.

(E) Representative immunofluorescent images showing no goat primary antibody controls for antibody feeding and total labeling of proteasome experiments. NF-H immunostaining (green) was used to mark neurons. Hoechst (blue) was used to label nuclei.

(F and G) Representative immunofluorescent images of DIV 6 cultured DRG neurons showing surface proteasome labeling using antibodies against the α2 (F) and β2 (G) proteasome subunits.
(H) Representative images showing total (cytoplasmic and membrane) labeling of proteasomes using an antibodies against the β5 proteasome subunit. Total labeling shows labeling on soma and axons of DRG neurons as well as labeling on the other cells cells present in the culture. NF-H immunostaining (green) was used to label neurons, and Hoechst (blue) labels nuclei.
(I) Representative images of cultured DRG neurons showing surface β5 proteasome subunit labeling co-stained with antibodies against GFAP to label glia cells and NF-H to label neurons. Bar graphs show the % of nuclei in the cultures that stained positive for GFAP, NF-H, nuclei that were not positive for either GFAP or NF-H ($Label^-$) and nuclei that were NMP positive (bar graph on the left). Bar graph on the right shows the % NMP positive nuclei that were also positive for NF-H and % NMP positive nuclei that were also positive for GFAP. Quantifications were calculated from multiple images per culture from at least three independent cultures. Each data point in these quantifications represents the observations from one image. Images for this experiment were acquired under the conditions that at least one cell in the field of view was positive for NMP and NF-H. Data are presented as mean ± SEM (n = 13 images analyzed).
(J) Representative images showing NMP localization (red) on neurons in all three major neuronal subgroups labeled with neurochemical markers for NF-H (green, top), CGRP (yellow, middle), and IB4 (cyan, bottom), but not in every neuron within subgroup. Nuclei are labeled with Hoechst (blue). Bar graphs on the left show the % neurons labeled with each neurochemical maker that were also positive for NMP and the % NMP positive neurons that were also labeled for each of the three neurochemical markers. Each data point in these quantifications represents observations from one image. Data are represented in mean ± SEM (n = 25 - 32 images analyzed).

(K) Bar graph scatterplot shows localization of NMP in different size soma. Data are presented as mean ± SEM (n = 20 images analyzed).

(L) Representative images of dual surface labeling for P2X3 receptor and β5 proteasome subunit on DIV 6 DRG neuron cultures. NF-H immunostaining (green) was used to label DRG neurons and Hoechst to label nuclei.

All DRG culture experiments represent at least three independent culture experiments where the cultures were obtained by dissecting and combining DRGs from four animals per culture.

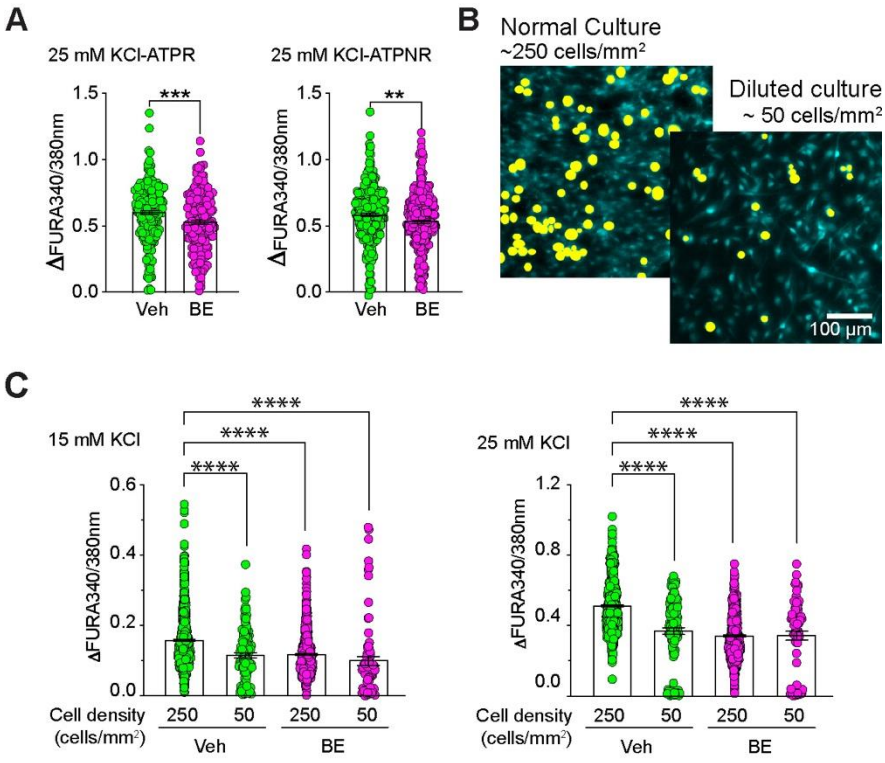
A
25 mM KCl-ATPR
25 mM KCl-ATPNR
ΔFURA340/380nm
1.5
1.0
0.5
0.0
***
**
Veh
BE
B
Normal Culture
~250 cells/mm²
Diluted culture
~ 50 cells/mm²
100 µm
C
15 mM KCl
25 mM KCl
ΔFURA340/380nm
0.6
0.4
0.2
0.0
1.2
0.8
0.4
0.0
****
Cell density
(cells/mm²)
250
50
250
50
Veh
BE

**Figure S5. Related to Figure 5.**

**The PNS NMP modulates neuronal responsiveness in a non-cell autonomous manner**

(A) Quantification of calcium imaging response to 25 mM KCl after pretreatment with αβ-meATP in αβ-meATP responsive neurons (ATPR) and αβ-meATP non-responsive neurons (ATPNR). Data are presented as mean ± SEM (n = 3 for vehicle and 4 for BE). **p < 0.01, ***p < 0.001 (one-way ANOVA with a Tukey's post hoc test).

(B) Representative images showing comparisons between normal density DRG (top) and low-density (bottom) cultures. Yellow circles represent individual DRG neurons.

(C) Calcium imaging responses to 15 and 25 mM KCl in normal (250) and diluted (50) density cultures. Quantifications show significantly reduced responses in normal cultures after BE treatment that were similarly reduced by diluting the cell density. BE treatment had no effect on stimulation response in diluted cultures. Data are presented as mean ± SEM (n = 4). ****p < 0.0001 (one-way ANOVA with a Tukey's post hoc test).

All DRG culture experiments represent at least three independent culture experiments where the cultures were obtained by dissecting and combining DRGs from four animals per culture.

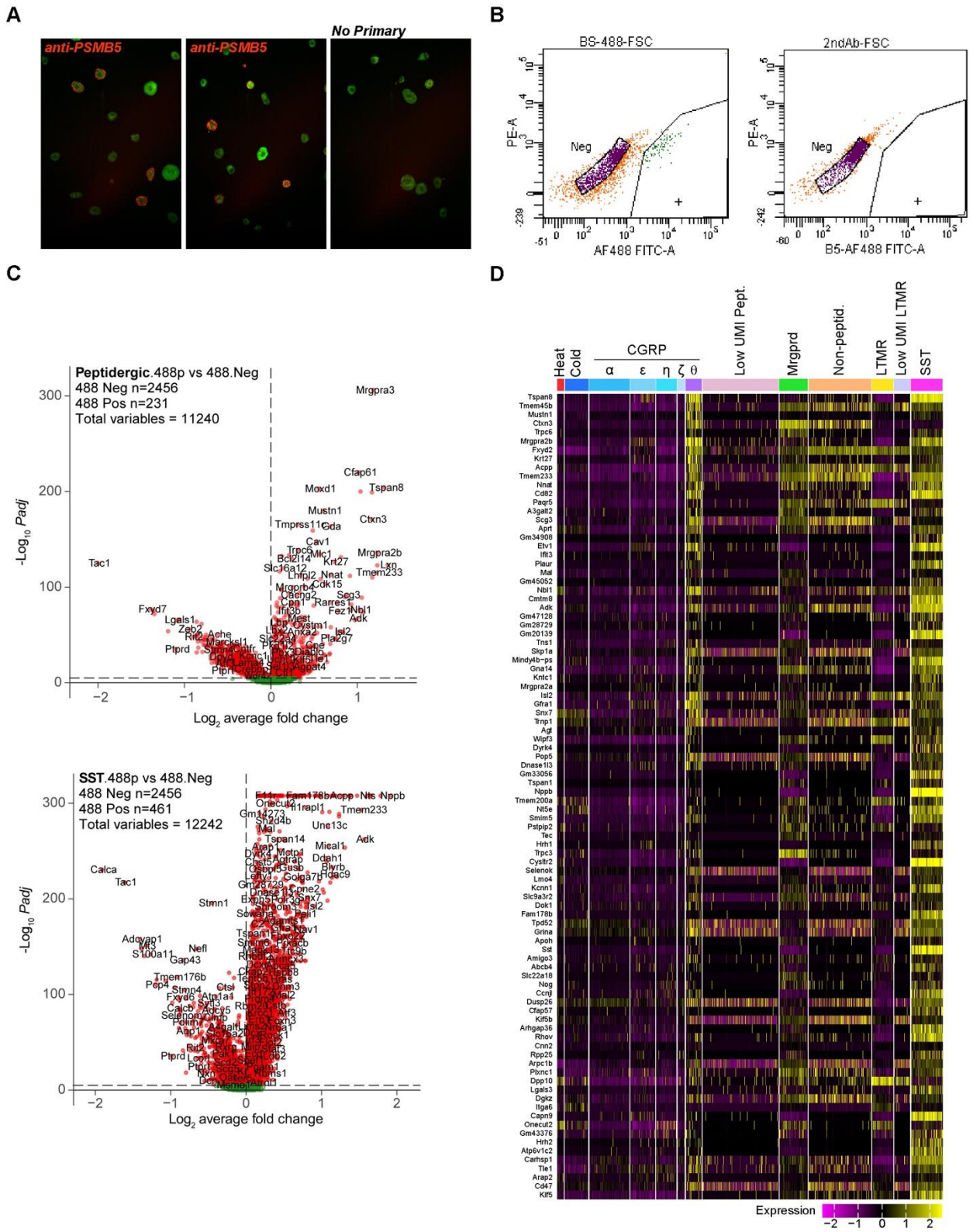
A
anti-PSMB5
anti-PSMB5
No Primary
B
BS-488-FSC
2ndAb-FSC
PE-A
Neg
+
AF488 FITC-A
B5-AF488 FITC-A
C
Peptidergic.488p vs 488.Neg
488 Neg n=2456
488 Pos n=231
Total variables = 11240
-Log10 Padj
Log2 average fold change
SST.488p vs 488.Neg
488 Neg n=2456
488 Pos n=461
Total variables = 12242
D
Heat
Cold
CGRP
α
ε
η
ζ
θ
Low UMI Pept.
Mrgprd
Non-peptid.
LTMR
Low UMI LTMR
SST
Expression

**Figure S6. Related to Figure 6 and Table S2, S3, and S4.**

**Single-cell RNA seq characterization of NMP positive neurons**

(A) Representative immunofluorescence images of dissociated DRG neurons showing cells that are positive (red) and negative for NMP labeled by antibody feeding using an antibody against the β5 proteasome subunit.

(B) Fluorescence-activated cell sorting (FACS) of dissociated DRG neurons that were labeled by antibody feeding. FACS plots show positive identification of cells that were 488-positive ($NMP^+$) from a larger pool of cells that are 488-negative. No primary antibody feeding control (right) shows no detection of cells that were 488-positive.

(C and D) Data from scRNA seq. (C) Volcano plots of differential gene expression comparisons of the NMP-positive peptidergic vs. NMP-negative peptidergic neurons (top) and NMP positive SST vs. all NMP-negative neurons (bottom). (D) Heatmap of top differentially expressed genes showing the top 100 genes that are specifically expressed in NMP-positive SST and CGRP-θ neurons. Expression scale shown at the bottom of the heatmap. Differential expression was performed comparing each cluster to all other cells in the data set using Mann-Whitney U test. Genes were selected by fold-change.

***No pretreatment***

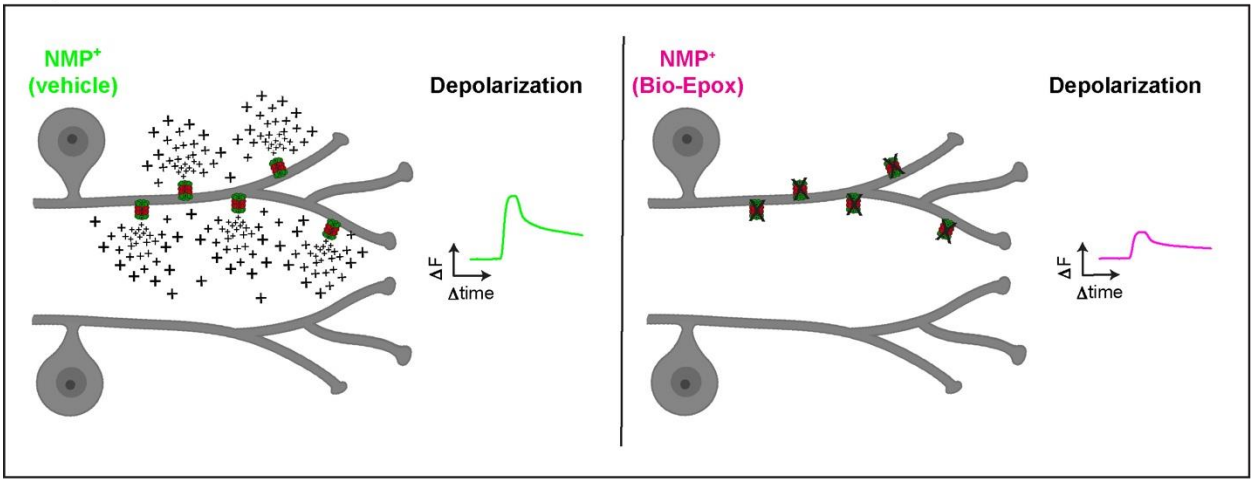


***Histamine pretreatment***

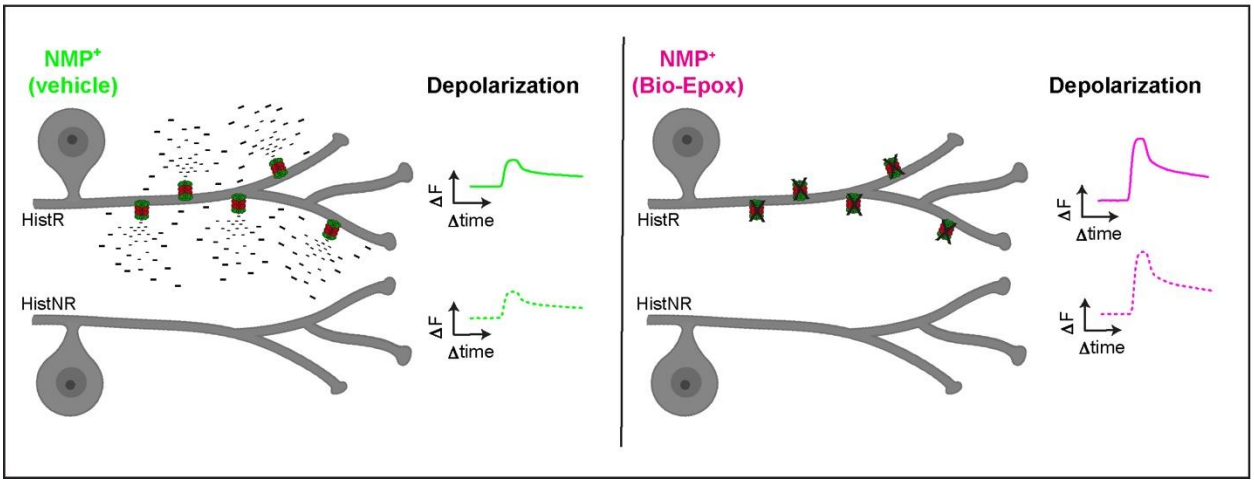

**Figure S7.**

**The PNS NMP is a mediator of somatosensory neuron 'crosstalk' that modulates context dependent response to stimulation**

Our data favors the following model. (Top left) Under baseline conditions (no pretreatment) $NMP^+$ neurons enhance the sensitivity to depolarization of all neighboring neurons (NMP expressing and NMP non-expressing). (Top right) This, we believe, occurs through the NMP as the addition of bio-epox, which inhibits the NMP, leads to decreased sensitivity to depolarization. (Bottom left) In contrast, pretreatment with histamine switches the $NMP^+$ neuron to inhibit the sensitivity to depolarization of all neighboring neurons (histamine responsive and histamine non-responsive). (Bottom Right) Again, we believe this occurs through the NMP as addition of bio-epox now leads to increased sensitivity to stimulation.